Spin Dimer and Electronic Band Structure Analyses of the Ferromagnetism versus Antiferromagnetism in $SeCuO_3$ and $TeCuO_3$

A. Villesuzanne,*[,†,||] M.-H. Whangbo,*[,†] M. A. Subramanian,[‡] and S. F. Matar[§]

Department of Chemistry, North Carolina State University, Raleigh, North Carolina 27695-8204, Dupont Central Research and Development, Experimental Station, Wilmington, Delaware 19880-0328, and ICMCB-CNRS, 87 Avenue Dr. Schweitzer, 33608 Pessac Cedex, France

Received April 26, 2005. Revised Manuscript Received June 28, 2005

On the basis of spin dimer analysis and density functional theory electronic band structure calculations, we examined why the magnetic ground state of $SeCuO_3$ is ferromagnetic while that of its isostructural analogue $TeCuO_3$ is antiferromagnetic and estimated their spin exchange parameters. The essential difference between the magnetic properties of these oxides arises from their Cu−O(1)−Cu superexchange, but not their Cu−O(2)−Cu superexchange. Spin exchange paths relevant for understanding magnetic properties are those that contain magnetic orbitals.

1. Introduction

The isostructural compounds $SeCuO_3$ and $TeCuO_3$ as well as their solid solution $Se_{1-x}Te_xCuO_3$ ($0 \le x \le 1$) possess a distorted perovskite structure in which the ∠Cu−O−Cu angles vary in the range of 120−130° due to the small size of the Q^{4+} (Q = Se, Te) ions and their covalent bonding with oxygen atoms.[1−3] The crystal structures of these compounds have two nonequivalent oxygen atoms, O(1) and O(2), and their distortion from the ideal perovskite structure is described by the ∠Cu−O(1)−Cu and ∠Cu−O(2)−Cu angles. The Cu−O(1)−Cu bridges run along the *b* direction, and the ∠Cu−O(1)−Cu angle of $Se_{1-x}Te_xCuO_3$ remains approximately constant around ∼123°. The Cu−O(2)−Cu bridges occur in the *ac* plane, and the ∠Cu−O(2)−Cu angle of $Se_{1-x}Te_xCuO_3$ increases gradually from 121° for $x = 0$ to 131° for $x = 1$.[3] As the temperature is lowered, $SeCuO_3$ undergoes a ferromagnetic (FM) ordering below $T_C = 25$ K, but $TeCuO_3$ undergoes an antiferromagnetic (AFM) ordering below $T_N = 7$ K.[3] The structural, magnetic susceptibility, and heat capacity studies showed that $Se_{1-x}Te_xCuO_3$ ($0 \le x \le 1$) undergoes a transition from an FM ground state ($x < \sim 0.4$) to an AFM ground state ($x > \sim 0.4$), and ∠Cu−O(2)−Cu = 127° ± 0.5° at the crossover point $x \approx 0.4$.[3] A sensitive dependence of magnetic properties on small structural changes has been observed for some vanadates, e.g., AV_4O_9 (A = Ca, Cs_2, DPP) and AV_2O_5 (A = Li, Na, Ca, Mg).[4]

In a magnetic oxide of transition-metal ions M possessing unpaired spins, the spin exchange interactions between adjacent metal ions are either of the superexchange (SE) type involving M−O−M paths or of the super-superexchange (SSE) type involving M−O···O−M paths. A qualitative guide for guessing the strengths of SE interactions[5−7] is provided by Goodenough rules, which allow one to rationalize the dependence of an SE interaction on the ∠M−O−M bond angle, the symmetry properties of the metal d orbitals containing unpaired spins, and the number of unpaired spins at the metal site M.[7] When a magnetic system has pairs of adjacent metal ions linked by different M−O−M bridges, it becomes difficult to know which bridge, and hence which pair of metal ions, is crucial for its magnetic properties. In the present work we examine why the magnetic properties of $SeCuO_3$ are different from those of $TeCuO_3$ by analyzing their spin exchange interactions on the basis of spin dimer analysis and density functional theory (DFT) electronic band structure calculations.

2. Crystal Structures and Spin Dimers of $QCuO_3$ (Q = Se, Te)

Each CuO_6 octahedron of $QCuO_3$ has two long (l), two medium (m), and two short (s) Cu−O bonds, which we denote as Cu−O(l), Cu−O(m), and Cu−O(s), respectively. The Cu−O(m) bonds are associated with the O(1) atoms and the Cu−O(l) and Cu−O(s) bonds with the O(2) atoms. The magnetic orbital of each axially elongated CuO_6 octahedron is contained in the $Cu(O_{eq})_4$ square plane made up of two Cu−O(s) and two Cu−O(m) bonds. The two Cu−O(m) bonds are *trans* to each other, and so are the two Cu−O(s)

† Department of Chemistry, North Carolina State University, Raleigh, North Carolina 27695-8204.
‡ Dupont Central Research and Development, Experimental Station, Wilmington, Delaware 19880-0328.
§ ICMCB-CNRS, 87 Avenue Dr. Schweitzer, 33608 Pessac Cedex, France.
|| Permanent address: ICMCB-CNRS, 87 Ave. Dr. Schweitzer, 33608 Pessac Cedex, France.

(1) Kohn, K.; Inoue, K.; Horie, O.; Akimoto, S. *J. Solid State Chem.* **1976**, *18*, 27.
(2) Philippot, E.; Maurin, M. *Rev. Chim. Miner.* **1976**, *13*, 162.
(3) Subramanian, M.; Ramirez, A. P.; Marshall, W. J. *Phys. Rev. Lett.* **1999**, *82*, 1558.
(4) (a) Whangbo, M.-H.; Koo, H.-J.; Dai, D. *J. Solid State Chem.* **2003**, *176*, 417. (b) Ueda, Y. *Chem. Mater.* **1998**, *10*, 2653. (c) Valentí, R.; Saha-Dasgupta, T.; Alvarez, J. V.; Požgajčić, K.; Gros, C. *Phys. Rev. Lett.* **2001**, *86*, 5381.
(5) Anderson, P. W. *Phys. Rev.* **1950**, *79*, 705.
(6) Goodenough, J. B. *Magnetism and the Chemical Bond*; Wiley: New York, 1963.
(7) Kanamori, J. *J. Phys. Chem. Solids* **1959**, *10*, 87.

10.1021/cm050885j CCC: $30.25
Published on Web 07/28/2005

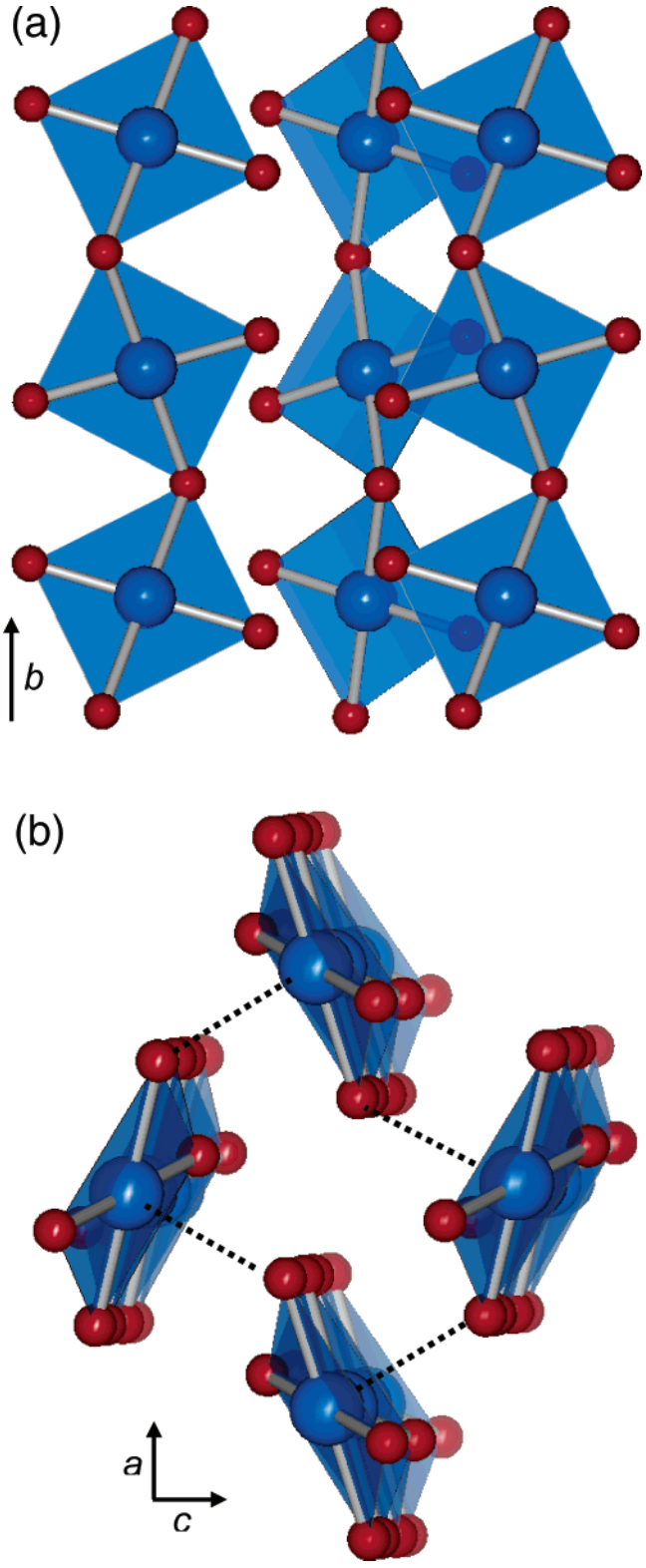

Figure 1. Arrangements of the $Cu(O_{eq})_3$ chains in $QCuO_3$ (Q = Se, Te), where the $Cu(O_{eq})_4$ square planes are defined in terms of the Cu−O(s) and Cu−O(m) bonds: (a) a perspective view of the $Cu(O_{eq})_3$ chains; (b) projection view of the $Cu(O_{eq})_3$ chains along the chain direction. The dotted lines represent the Cu−O(l) bonds between adjacent $Cu(O_{eq})_3$ chains. For simplicity, only one Cu−O(l) bond is shown between adjacent chains.

bonds. If the local coordinates of each CuO_6 octahedron are defined such that the *x* and *y* axes run approximately along the Cu−O(m) and Cu−O(s) bonds, respectively, the magnetic orbital of each CuO_6 octahedron is described as the Cu $d_{x^2-y^2}$ orbital that has the equatorial oxygen p orbitals

Table 1. Geometrical Parameters Associated with the SE Path Cu−O−Cu and the SSE Path Cu−O···O−Cu of $QCuO_3$ (Q = Se, Te)

	type	N^a	param[b]	$SeCuO_3$	$TeCuO_3$
J_b	Cu−O(1)−Cu along *b*	2	Cu−O	2.090	2.055
			∠Cu−O−Cu	122.4	123.9
			Cu···Cu	3.663	3.628
J_{ac}	Cu−O(2)−Cu in the *ac* plane	4	Cu−O	2.251, 1.919	2.600, 1.925
			∠Cu−OCu	127.1	129.5
			Cu···Cu	3.984	4.102
J_1'	Cu−O···O−X*v* in the *ac* plane	4	Cu−O	2.090, 1.919	2.055, 1.925
			O···O	2.695	2.941
			∠Cu−O···O	147.0, 99.9	146.0, 99.0
			Cu···Cu	5.412	5.476
J_2'	Cu−O···O−X*v* in the *ac* plane	4	Cu−O	1.919, 2.090	1.925, 2.055
			O···O	3.385	3.593
			∠Cu−O···O	122.6, 90.2	124.8, 88.6
			Cu···Cu	5.412	5.476
J_3'	Cu−O···O−X*v* along *a*	2	Cu−O	1.919, 1.919	1.925, 1.925
			O···O	2.817	2.754
			∠Cu−O···O	126.7, 126.7	128.5, 128.5
			Cu···Cu	5.965	5.967

[a] The number of equivalent spin exchange paths from a given Cu atom. [b] Bond lengths and bond angles are given in units of angstroms and degrees, respectively.

combined out-of-phase to make a σ antibonding interaction with the Cu $d_{x^2-y^2}$ orbital. The $Cu(O_{eq})_4$ square planar units form a $Cu(O_{eq})_3$ chain along the *b* axis by sharing their O(m) atoms (Figure 1a). When the Cu−O(l) bonds are added to each $Cu(O_{eq})_4$ square plane, we obtain a corner-sharing CuO_5 chain from a corner-sharing $Cu(O_{eq})_3$ chain. The adjacent CuO_5 chains share their oxygen corners to form the three-dimensional CuO_3 lattice. In this interchain corner-sharing, the O(s) atoms of one CuO_5 chain become the O(l) atoms of the adjacent CuO_5 chains (Figure 1b). Table 1 summarizes the structural parameters of several spin exchange paths of $QCuO_3$ (Q = Se, Te). A given Cu atom has two Cu−O(1)−Cu paths along the *b* direction (J_b), four Cu−O(2)−Cu paths in the *ac* plane (J_{ac}), four Cu−O···O−Cu paths in the *ac* plane (J_1'), four Cu−O···O−Cu paths in the *ac* plane (J_2'), and two Cu−O···O−Cu paths along the *a* direction (J_3').

3. Spin Dimer Analysis

In spin dimer analysis[8] based on extended Hückel tight binding (EHTB)[9] calculations, the trend in the spin exchange parameters $J = J_F + J_{AF}$ is examined by considering the trend in their AFM components J_{AF}. As discussed in the previous section, the spin dimers important for $QCuO_3$ (Q = Se, Te) are the Cu_2O_7 dimers made up of two corner-sharing $Cu(O_{eq})_4$ square planes. Provided that the two spin sites 1 and 2 of a spin dimer are described by magnetic orbitals ϕ_1 and ϕ_2, respectively, their interaction leads to the levels ψ_+ and ψ_- of the spin dimer with energy separation of Δe. Then the J_{AF} term is written as[8]

$$J_{AF} = -(\Delta e)^2/U_{eff} \quad (1)$$

where U_{eff} is the effective on-site repulsion. In general, U_{eff} is nearly constant for a series of closely related systems so that a trend in J_{AF} values is well reproduced by that in the

(8) For recent reviews, see ref 4a and Whangbo, M.-H.; Dai, D.; Koo, H.-J. *Solid State Sci.* **2005**, *7*, 827.
(9) Our calculations were carried out by employing the SAMOA (Structure and Molecular Orbital Analyzer) program package (Dai, D.; Ren, J.; Liang, W.; Whangbo, M.-H. http://chvamw.chem.ncsu.edu/, 2002).

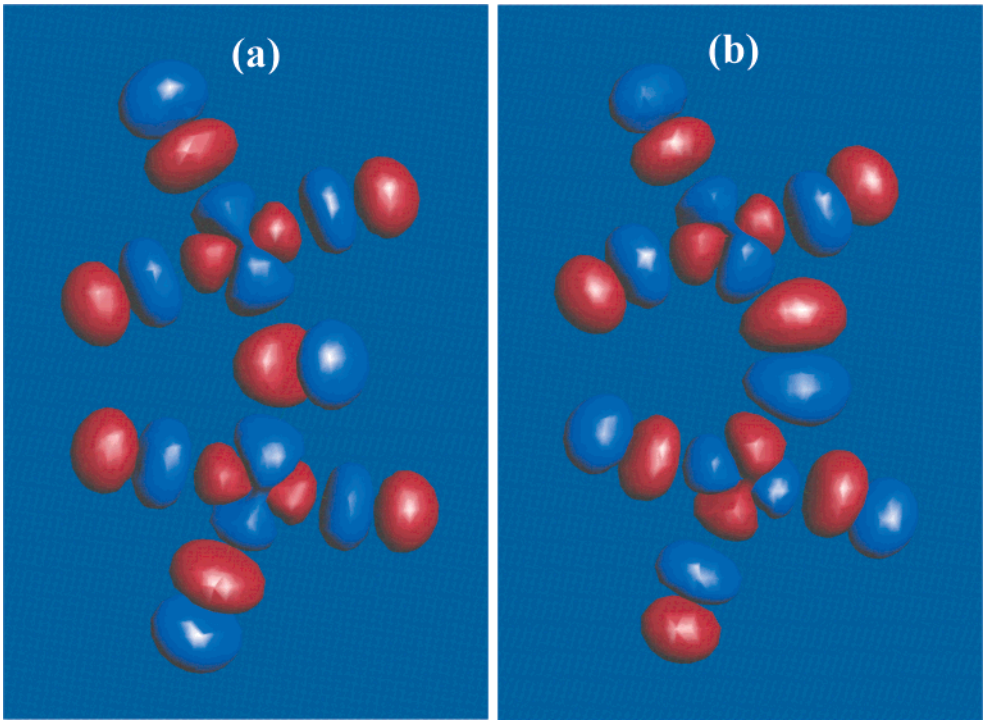

Figure 2. (a) ψ_+ and (b) ψ_- orbitals of the spin dimer Cu_2O_7 arising from the interaction between the two magnetic orbitals ϕ_1 and ϕ_2 at the two spin sites.

corresponding $-(\Delta e)^2$ values. In general, the FM component, J_F, is a small positive number so that the trend in the $-(\Delta e)^2$ values reflects that in the corresponding J values. The magnetic orbitals ψ_+ and ψ_- of the spin dimer Cu_2O_7 are shown in parts a and b, respectively, of Figure 2. In the Cu−O−Cu bridge of this spin dimer, the Cu $d_{x^2-y^2}$ orbitals make a stronger antibonding interaction with the O 2p orbital in ψ_- than in ψ_+ so that Δe is nonzero. The $(\Delta e)^2$ values calculated for the spin exchange interaction J_b of $QCuO_3$ (Q = Se, Te) show that the tendency for AFM coupling is stronger in $TeCuO_3$ than in $SeCuO_3$ [i.e., $(\Delta e)^2 = 0.073$ vs 0.053 $(eV)^2$]. This result is consistent with the geometrical features of the SE paths; namely, the Cu−O(m) bond is shorter and the ∠Cu−O(m)−Cu angle is larger in $TeCuO_3$ than in $SeCuO_3$. The $(\Delta e)^2$ values calculated for other spin exchange interactions (i.e., J_{ac}, J_1', J_2', and J_3') are negligible compared with those calculated for the J_b interaction (i.e., smaller than 2%). Thus, it is expected that the J_{ac}, J_1', J_2', and J_3' interactions are either weakly antiferromagnetic or ferromagnetic.

4. Spin-Polarized Electronic Band Structure Analysis of Ordered Spin States

The four ordered spin arrangements of interest for $QCuO_3$ (Q = Se, Te) are the FM, the A-type antiferromagnetic (A-AFM), the C-type antiferromagnetic (C-AFM), and the G-type antiferromagnetic (G-AFM) arrangements. The A-AFM arrangement represents an AFM ordering of ferromagnetically ordered planes (here the *ac* planes), the C-AFM arrangement an AFM ordering of ferromagnetically ordered chains (here along the *b* direction), and the G-AFM arrangement an AFM ordering in all three crystallographic directions (Figure 3). We examine the relative stabilities of these four ordered spin arrangements on the basis of spin-polarized DFT electronic structure calculations using the full-potential linearized augmented plane wave plus local orbitals (L/APW+lo) method[10,11] implemented in the WIEN2k package.[12]

In our spin-polarized DFT calculations for these ordered spin arrangements, the spin directions of the Cu sites were constrained but those of the oxygen sites were not. We used the generalized gradient approximation (GGA) of Perdew, Burke, and Ernzerhof for the exchange-correlation potential.[13] The atomic sphere radii used were 2.08 au for Te, 1.7 au for Se, 2.0 au for Cu, and 1.5 au for O. Up to 500 *k* points were employed for the Brillouin zone sampling. Self-consistency was achieved to a precision below 0.5 meV for the total energy per formula unit (FU). The crystal structures of $SeCuO_3$ and $TeCuO_3$ used for our calculations are those employed in the spin dimer analysis. To check the possible effects of electron correlation, we also carried out LDA+U[14,15] calculations within the L/APW scheme for the FM and A-AFM states of $SeCuO_3$ and $TeCuO_3$ with parameters U = 8 eV and J = 1 eV for the Cu 3d orbitals.

The relative energies of the FM, G-AFM, C-AFM, and A-AFM states obtained from our GGA calculations are summarized in Table 2. In $SeCuO_3$ the FM state is more

(10) Sjöstedt, E.; Nordström, L.; Singh, D. *Solid State Commun.* **2000**, *114*, 15.
(11) Madsen, G. K. H.; Blaha, P.; Schwarz, K.; Sjöstedt, E.; Nordström, L. *Phys. Rev. B* **2001**, *64*, 195134.
(12) Blaha, P.; Schwarz, K.; Madsen, G. K. H.; Kvasnicka, D.; Luitz, J. *WIEN2k, An Augmented Plane Wave Plus Local Orbitals Program for Calculating Crystal Properties*; Vienna University of Technology: Vienna, Austria, 2001.
(13) Perdew, J. P.; Burke, K.; Ernzerhof, M. *Phys. Rev. Lett.* **1996**, *77*, 3865.
(14) Anisimov, V. I.; Solovyev, I. V.; Korotin, M. A.; Czyzyk, M. T.; Sawatzky, G. A. *Phys. Rev. B* **1993**, *48*, 16929.
(15) Liechtenstein, A. I.; Anisimov, V. I.; Zaanen, J. *Phys. Rev. B* **1995**, *52*, R5467.

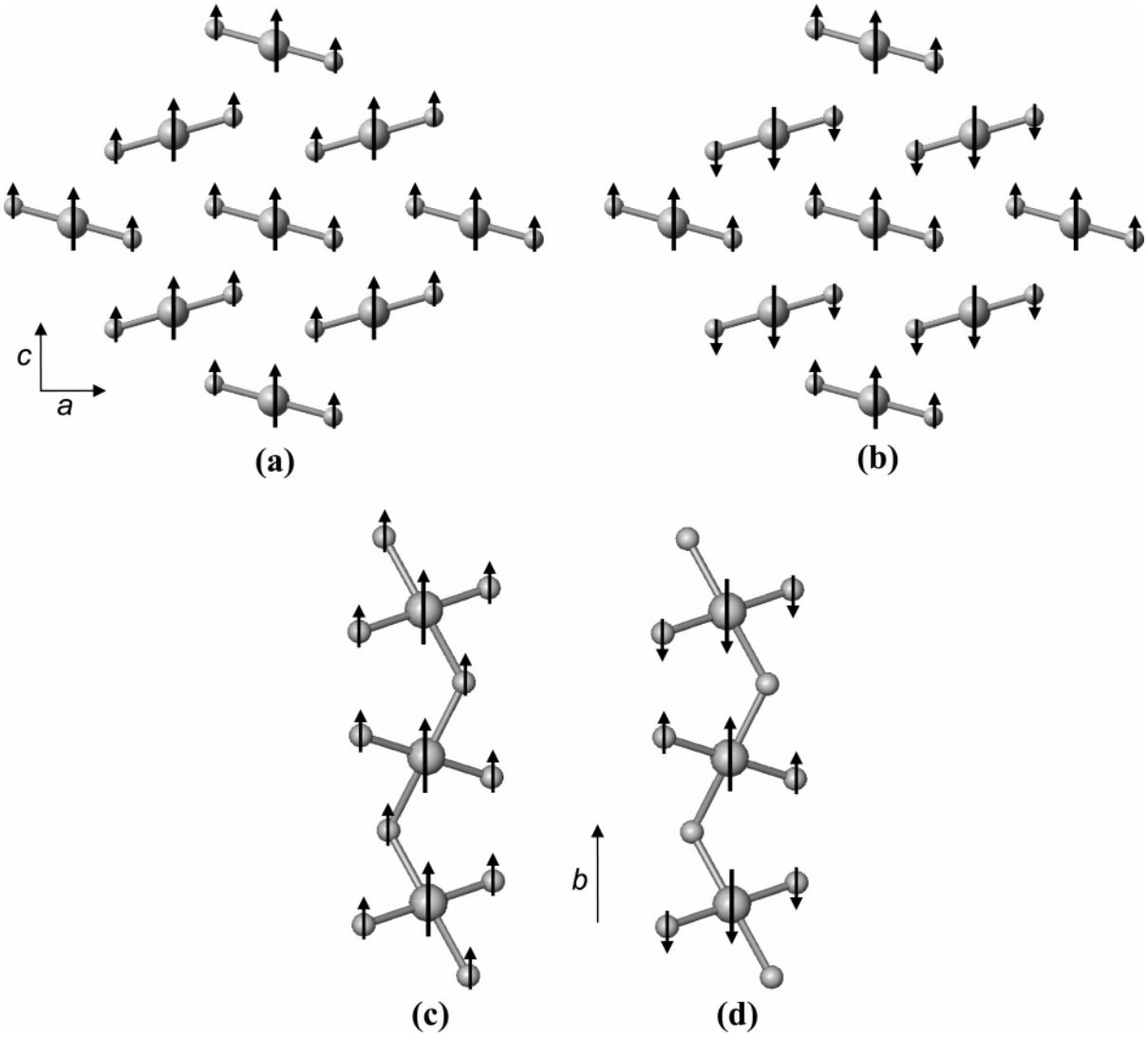

Figure 3. Schematic diagrams describing the ordered spin arrangements FM, A-AFM, C-AFM, and G-AFM of $QCuO_3$: (a) a projection view along the chain direction of the ferromagnetically ordered $Cu(O_{eq})_3$ chains in the *ac* plane, where the O(m) atoms are not shown for simplicity; (b) a projection view of the antiferromagnetically ordered $Cu(O_{eq})_3$ chains in the *ac* plane, where the O(m) atoms are not shown for simplicity; (c) a perspective view of a ferromagnetically ordered $Cu(O_{eq})_3$ chain; (d) a perspective view of an antiferromagnetically ordered $Cu(O_{eq})_3$ chain.

Table 2. Relative Energies ΔE and Unpaired Spin Populations on the Cu and O Atoms of $QCuO_3$ (Q = Se, Te) Obtained from GGA Calculations with the L/APW+lo Method

			net spin population		
compd	state	ΔE^a	Cu	O(1)	O(2)
$SeCuO_3$	FM	0	+0.60	+0.15	+0.08
	A-AFM	+9	±0.57	±0.00	±0.05
	C-AFM	+12	±0.58	±0.12	±0.06
	G-AFM	+12	±0.55	±0.00	±0.07
$TeCuO_3$	FM	0	+0.60	+0.14	+0.09
	A-AFM	−7	±0.56	±0.00	±0.05
	C-AFM	+8	±0.58	±0.12	±0.06
	G-AFM	−6	±0.54	±0.00	±0.06

[a] ΔE values are in millielectronvolts per formula unit.

stable than all the AFM states. In $TeCuO_3$ the A-AFM and G-AFM states are more stable than the FM state, which is in turn more stable than the C-AFM state. The same trends were obtained from our LDA+*U* calculations, with the energy difference $E_{A-AFM} - E_{FM} = +1.5$ and -2.0 meV per FU for $SeCuO_3$ and $TeCuO_3$, respectively. These results are consistent with both experiment and spin dimer analysis. As can be seen from Figure 3, the Cu and O_{eq} atoms of a $Cu(O_{eq})_4$ square plane carry the same kind of spin densities due to the nature of its $d_{x^2-y^2}$ magnetic orbital. For symmetry reasons, the spin density on the O(m) atom vanishes for the states with AFM ordering along the *b* axis. For simplicity, the total and partial density of states (DOS) plots calculated from our GGA calculations are presented only for the FM and A-AFM states of $QCuO_3$ in Figures 4 and 5, respectively. As expected, the unpaired spin density on each copper site arises mainly from the occupied up-spin band of the $d_{x^2-y^2}$ orbital character. The empty down-spin band of the $d_{x^2-y^2}$ orbital character has a larger width for $TeCuO_3$ than for $SeCuO_3$. This shows that the interactions between adjacent $d_{x^2-y^2}$ orbitals through the Cu−O(m)−Cu bridges in the $Cu(O_{eq})_3$ chains are stronger in $TeCuO_3$ than in $SeCuO_3$, which is understandable because $TeCuO_3$ has a larger ∠Cu−O(m)−Cu angle and a shorter Cu−O(m) bond than does $SeCuO_3$.

5. Spin Exchange Parameters

On the basis of the relative energies of the FM, A-AFM, C-AFM, and G-AFM states described in the previous section, we now estimate the spin exchange parameters (i.e., J_b, J_{ac}, J_1', J_2', and J_3') of $QCuO_3$. With the energies of four different

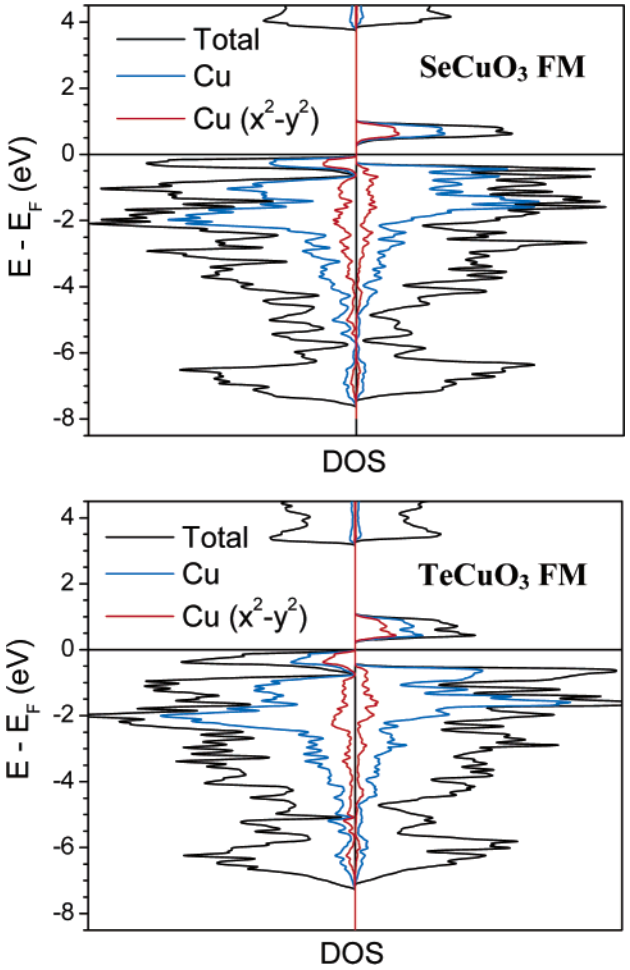

Figure 4. Total and partial DOS plots for the FM state of $SeCuO_3$ and $TeCuO_3$ obtained from GGA calculations with the L/APW+lo method. The left- and right-hand side panels refer to the up-spin and down-spin states, respectively.

ordered spin states, only three exchange parameters can be estimated. If the two SSE parameters J_1' and J_2' are assumed to be equal (i.e., $J_1' = J_2' = J'$), the energies of the FM, A-AFM, C-AFM, and G-AFM states are expressed in terms of the exchange parameters J_b, J_{ac}, J', and J_3' as[8,16]

$$\begin{aligned} E_{\mathrm{FM}} &= -J_b - 2J_{ac} - 4J' - J_3' \\ E_{\mathrm{A-AFM}} &= J_b - 2J_{ac} + 4J' - J_3' \\ E_{\mathrm{C-AFM}} &= -J_b + 2J_{ac} + 4J' - J_3' \\ E_{\mathrm{G-AFM}} &= J_b + 2J_{ac} - 4J' - J_3' \end{aligned} \qquad (2)$$

which lead to the three energy differences

$$\begin{aligned} \Delta E_{\mathrm{A}} &= E_{\mathrm{A-AFM}} - E_{\mathrm{FM}} = 2J_b + 8J' \\ \Delta E_{\mathrm{C}} &= E_{\mathrm{C-AFM}} - E_{\mathrm{FM}} = 4J_{ac} + 8J' \\ \Delta E_{\mathrm{G}} &= E_{\mathrm{G-AFM}} - E_{\mathrm{FM}} = 2J_b + 4J_{ac} \end{aligned} \qquad (3)$$

where the J_3' term does not appear. From eq 3, the parameters J_b, J_{ac}, and J' are related to the energy differences as

$$\begin{aligned} J' &= -(\Delta E_{\mathrm{G}} - \Delta E_{\mathrm{C}} - \Delta E_{\mathrm{A}})/16 \\ J_b &= \Delta E_{\mathrm{A}}/2 - 4J' \\ J_{ac} &= \Delta E_{\mathrm{C}}/4 - 2J' \end{aligned} \qquad (4)$$

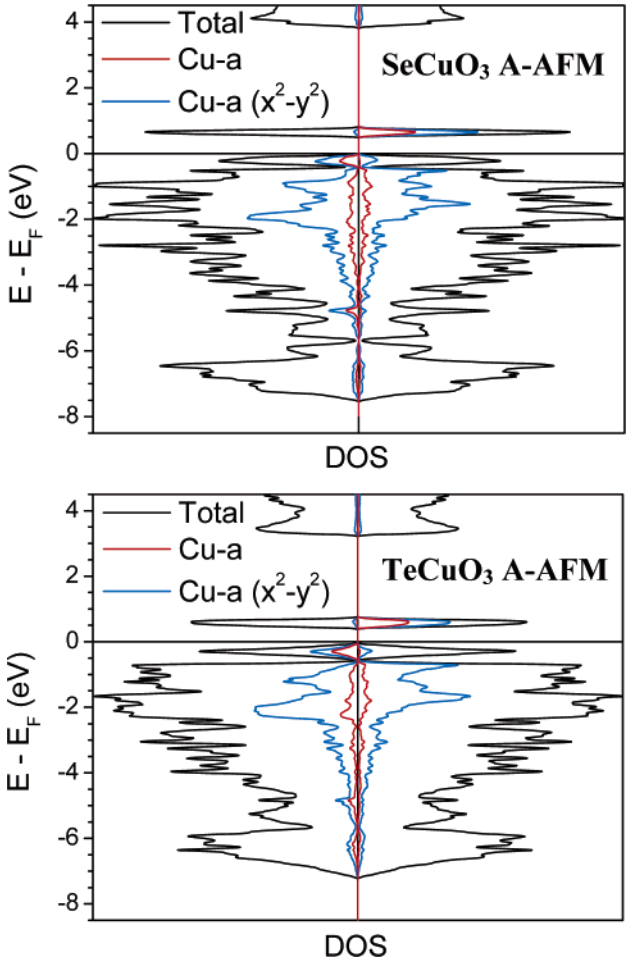

Figure 5. Total and partial DOS plots for the A-AFM state of $SeCuO_3$ and $TeCuO_3$ obtained from GGA calculations with the L/APW+lo method. The partial DOS is shown only for the spin-up Cu atoms (Cu-a). The left- and right-hand side panels refer to the up-spin and down-spin states, respectively.

Table 3. Values of the Spin Exchange Parameters (meV) of $QCuO_3$ (Q = Se, Te) Estimated from GGA Calculations with the L/APW+lo Method

param	$SeCuO_3$	$TeCuO_3$
J_b	+2.0	−5.4
J_{ac}	+1.9	+1.2
J'	+0.6	+0.5

By employing the energy differences ΔE_{A}, ΔE_{A}, and ΔE_{A} determined from our electronic band structure calculations (Table 2), the spin exchange parameters J_b, J_{ac}, and J' are estimated as listed in Table 3. Note that the J_3' value cannot be estimated from the four ordered spin states considered above. As expected from our spin dimer analysis of section 2, the parameters J_{ac} and J' are FM in both $SeCuO_3$ and $TeCuO_3$. The two compounds are different mainly in their SE interaction J_b through the Cu−O(1)−Cu bridges; namely, J_b is ferromagnetic in $SeCuO_3$ but antiferromagnetic in $TeCuO_3$.

6. Concluding Remarks

The present spin-polarized electronic band structure calculations correctly predict that the magnetic ground state of

(16) Dai, D.; Whangbo, M.-H. *J. Chem. Phys.* **2001**, *114*, 2887; **2003**, *118*, 29.

$SeCuO_3$ is FM and that of $TeCuO_3$ is AFM. Our electronic structure calculations show that the ground state of $TeCuO_3$ is either an A-AFM or a G-AFM type, but not a C-AFM type. Our crystal structure and spin dimer analyses of $QCuO_3$ (Q = Se, Te) show that the magnetic orbitals are contained in the $Cu(O_{eq})_4$ planes of their $Cu(O_{eq})_3$ chains, and hence, the essential difference between the magnetic properties of $SeCuO_3$ and $TeCuO_3$ arises from the difference in the Cu−O(m) bond lengths and the −Cu−O(m)−Cu bond angles of their $Cu(O_{eq})_3$ chains. As pointed out in recent studies,[8,17] it is important to recall that the spin exchange paths crucial for understanding magnetic properties are those that contain magnetic orbitals.

Acknowledgment. The work at North Carolina State University was supported by the Office of Basic Energy Sciences, Division of Materials Sciences, U.S. Department of Energy, under Grant DE-FG02-86ER45259. We thank the Pole M3PEC, Bordeaux 1 University, France, for computing resources.

CM050885J

(17) Whangbo, M.-H.; Koo, H.-J.; Dai, D.; Jung, D. *Inorg. Chem.* **2003**, *42*, 3898.